Sedimentology (1998) **45**, 1105–1124

Pedogenic-phreatic carbonates on a Middle Devonian (Givetian) terrigenous alluvial-deltaic plain, Gilwood Member (Watt Mountain Formation), northcentral Alberta, Canada

C. A. WILLIAMS* and F. F. KRAUSE
Department of Geology and Geophysics, University of Calgary, 2500 University Drive NW, Calgary, Alberta, Canada T2N 1N4 (E-mail: cwilliams@suncor.com, krause@geo. ucalgary. ca)

ABSTRACT

In the Muskeg Trough of northcentral Alberta the Gilwood Member contains widespread carbonate deposits that formed within terrigenous mudstone and sandstone hosts. Stratigraphic, depositional and petrographic relationships indicate that these carbonates represent calcretes and dolocretes. Calcretes, observed best with cathodoluminescence, display microcrystalline alpha fabrics, circumgranular cracks, root networks, displacive growth fabrics, elongate channel voids and rare coloform growths with flower spar. Similarly, dolocretes have microcrystalline alpha fabrics, brecciation, gradational contacts with host mudstones, extensive layered nodular horizons and are associated with anhydrite and pyrite. $\delta^{13}C$ values range between −7‰ to +1‰ and −6‰ to +3‰ for calcretes and dolocretes, respectively. Oxygen isotopes are more variable and differ with host lithologies. $\delta^{18}O$ of calcretes ranges between −11‰ to −8‰ for sandstones and −8‰ to −3‰ for mudstones, whereas $\delta^{18}O$ of dolocretes ranges between −3‰ to 1‰ for marine mudstones and −6‰ to −2‰ for pedogenic mudstones. Regional mapping indicates that calcretes thicken towards the deepest parts of the Muskeg Trough. Widespread dolocretes extend beyond the eastern and western limits of Muskeg Trough and are useful marker intervals for regional correlations. Dolocretes of restricted lateral extent are found within gleyed palaeosol mudstones next to calcretized channel sandstones.

Calcrete isotopic values are interpreted as indicative of carbonate precipitation from waters with meteoric water input. However, the higher $\delta^{18}O$ values in dolocretes are indicative of a contribution from an isotopically heavier source such as seawater. Stratigraphically, calcretes are most common along the western and northern edges of Muskeg Trough; thus, calcrete accumulation was further controlled by meteoric water in-flow from the highland to the west and sluggish groundwater flow in Muskeg Trough. In contrast, regionally widespread dolocrete horizons appear to have formed from mixing of fresh waters derived from the highland to the west and seawaters introduced from the east. Regionally restricted dolocretes which are found next to channel sandstones formed from groundwater out-flow from the permeable channel sandstones which resulted in calcretization in channel proximal mudstones and dolomitization in channel distal mudstones.

*Present address: Suncor Inc. Resources Group, 112 4 Ave SW, PO Box 38, Calgary, Alberta, Canada, T2P 2V5.

INTRODUCTION

Calcretes and dolocretes are commonly associated with both soil horizons and palustrine deposits. Several different interpretations have been published regarding their origin and geological significance (Gile *et al.*, 1966; Goudie, 1973; Arakel, 1986; El-Sayed *et al.*, 1991; Wright & Tucker, 1991). Important issues that are key to understanding the genesis of these carbonates have been uncovered by a number of researchers over the past three decades, namely: (1) are such carbonates vadose, pedogenic and/or phreatic in origin? (Strakhov, 1970; Netterberg, 1969; Thortenson *et al.*, 1972; Arakel, 1986; Land, 1970; Freytet & Plaziat, 1982; Molenaar, 1984; Spötl & Wright, 1992; Pimentel *et al.*, 1996); (2) is biological or microbial/fungal activity critical in their inception and subsequent development? (Klappa, 1980; Wright & Tucker, 1991; Wright *et al.*, 1995); and (3) were they the product of precipitation from supersaturated solutions where carbonate was contributed from aeolian dust, airborne salts, seasonal wetting, leaching and drying, and/or interaction with clays? (Sehgal & Stoops, 1972; Wieder & Yaalon, 1974; Yaalon & Singer, 1974; Watts, 1978; Chadwick & Nettleton, 1990).

In our study of the dominantly siliciclastic deposits of the Middle Devonian (Givetian) Gilwood Member (Watt Mountain Formation), we have found both ubiquitous calcretes and dolocretes, that are in part associated with gleysols and calcisols (as defined by Mack *et al.*, 1993). These carbonates appear to contain features that are pedogenic, vadose and/or phreatic in origin (see reviews in Esteban & Klappa, 1983; Tucker & Wright, 1990; Wright & Tucker, 1991). Further, unlike previous studies (El-Sayed *et al.*, 1991; Spötl & Wright, 1992), the lithology and composition of the host material of the Gilwood Member appears to have controlled the mineralogy of the nodule formed; calcretes are found in both mudstone and sandstone hosts, whereas dolocretes are present only in mudstones. Our primary objective was to determine the origin of these carbonates by combining sedimentological evidence with textural and fabric evidence, crystal morphology, cathodoluminescence, and isotope signatures. Secondly, we sought a reason for the dolocretes being present only in mudstones, whereas calcretes were present in all host lithologies.

Geologic setting

This study is based on cores from the Nipisi oil field, located in northcentral Alberta, Canada (Fig. 1). Reservoir sandstones of the Gilwood Member comprise a thin (<40 m), deltaic, siliciclastic wedge that is over-and underlain by mudstones of the Watt Mountain Formation. The Watt Mountain Formation is enclosed in impermeable evaporitic and carbonate sediments of the underlying Muskeg Formation and overlying Fort Vermilion Formation (Fig. 1). These bounding evaporitic units were deposited in the Elk Point Basin (Klingspor, 1969; Moore, 1989; Oldale & Munday, 1994; Meijer-Drees, 1994), which was near the equator during the Givetian (Witzke & Heckel, 1988; Scotese *et al.*, 1981; Ziegler, 1988; Moore, 1989). The palaeoclimate has been described as arid (Schuchert, 1976; Moore, 1989) with north-easterly equatorial trade winds (Habicht, 1979).

Major tectonic and depositional elements (Fig. 2) were: (1) the east to north-east trending Peace River Arch island archipelago, an elevated high grade metamorphic and igneous complex that was the main source of sediments comprising the Gilwood Member (Burwash, 1957; Pugh, 1973); (2) the Hay River and Western carbonate platforms to the north and west, respectively; (3) the Alberta/Saskatchewan carbonate ramps of the Elk Point Basin to the south and east; and (4) the north–south trending Muskeg Trough and Lake Muskeg in the Nipisi field area, a topographic low attributed to loss of underlying salts in the Muskeg Formation (Thachuk, 1968; Alcock & Benteau, 1976; Moore, 1989). Relative sea-level fluctuations created conditions varying from complete connection to complete isolation of the coastal Lake Muskeg from the seawater to the east (Fig. 3).

METHODS

Lithofacies analysis and mapping was based on detailed logging of 110 drill cores (Fig. 1) and correlation of ≈800 well logs. Thin section petrography, scanning electron microscopy (SEM) and X-ray diffraction (XRD) were used to determine bulk and clay mineralogy. X-ray diffraction was done using a CuK_{α} source, and glycolation, heating and drying techniques following Moore & Reynolds (1989). Thin sections were stained with Alizarin Red S and potassium ferricyanide to distinguish calcite from dolomite and to determine

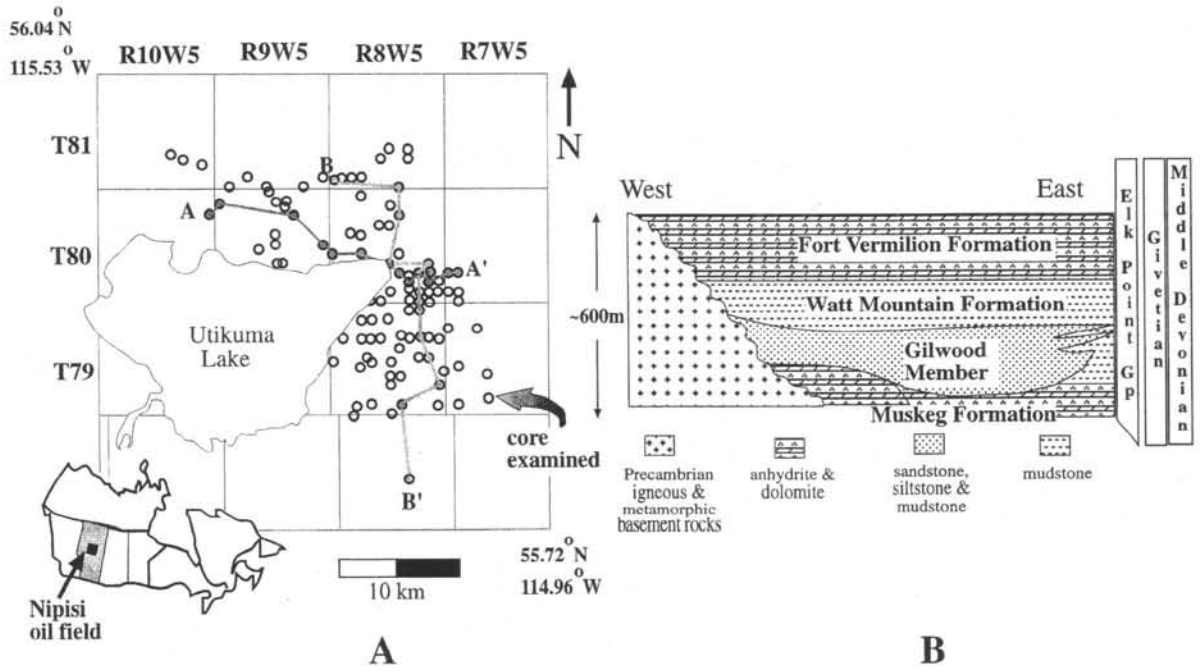

Fig. 1. (A) Study area in Alberta, Canada, with an enlarged map of all the cores examined in this study and the cross-sections displayed in Fig. 10. (B) West to east schematic cross-section of the Gilwood Member in the study area and its relationship to underlying and overlying rock units (not to scale), with chronostratigraphic and lithostratigraphic units (adapted from Oldale & Munday, 1994 and Meijer-Drees, 1994).

iron content. Cathodoluminescence petrography (CL) was done using a Luminoscope cold cathode source, at an operating range of 14–16 kV, 0·4–0·6 mA, 6–8 Pa vacuum and a beam diameter of 6–8 mm.

Stable carbon and oxygen isotope analyses were made on samples from seven cores in a north–south and east–west transect (Fig. 1). Analyses were made using the methods of McCrea (1950), and are reported in standard δ notation relative to the PDB standard. Values have standard deviations of 0·03‰ and 0·1‰ for carbon and oxygen, respectively. Calcite analyses were made on CO_2 evolved from an one hour dissolution in 100% H_3PO_4 at 20°C. The reaction vessel was then left for three days and the CO_2 evolved taken to reflect reaction from dolomite.

RESULTS

Observations from core

Calcretes

Nodular calcretes formed in both sandstones and mudstones of the Gilwood Member. Nodule morphology, size and characteristics are similar throughout the study area, with no pronounced systematic lateral or vertical variations. Pedogenic features associated with calcretized lithologies are: (1) red, green and gold colour mottling; (2) sediment infilled, V-shaped mud cracks, commonly 1–3 cm, but rarely up to 20 cm deep; (3) illuviation fabrics outlined by clays that have been washed downwards through porous lithology; and (4) rooting, commonly 1–5 cm, but rarely up to 20 cm deep. Calcretization is most common in green-grey mudstones or muddy sandstones that may be so pervasively cemented that gleying and other pedogenic features are poorly preserved.

Calcretes are nodular, with a wide range of sizes and shapes, from <1–>8 cm, with nodules oriented with both horizontal and vertical elongation (Fig. 4). Nodules within sandstones and shaly sandstones are associated with drab green to green grey haloes and both enclose and displace the host material; rare, vertical forms, up to 20 cm long, taper and branch downward. In contrast, within mudstones, nodules do not incorporate the surrounding sediment, but have sharp edges where clays are pushed into crenulate, tortuous, internodular spaces. This creates mosaics and stacks of alternating carbonate/mudstone layers. Mudstone colour within nodular sections is almost always green or rarely, green with red colour mottling.

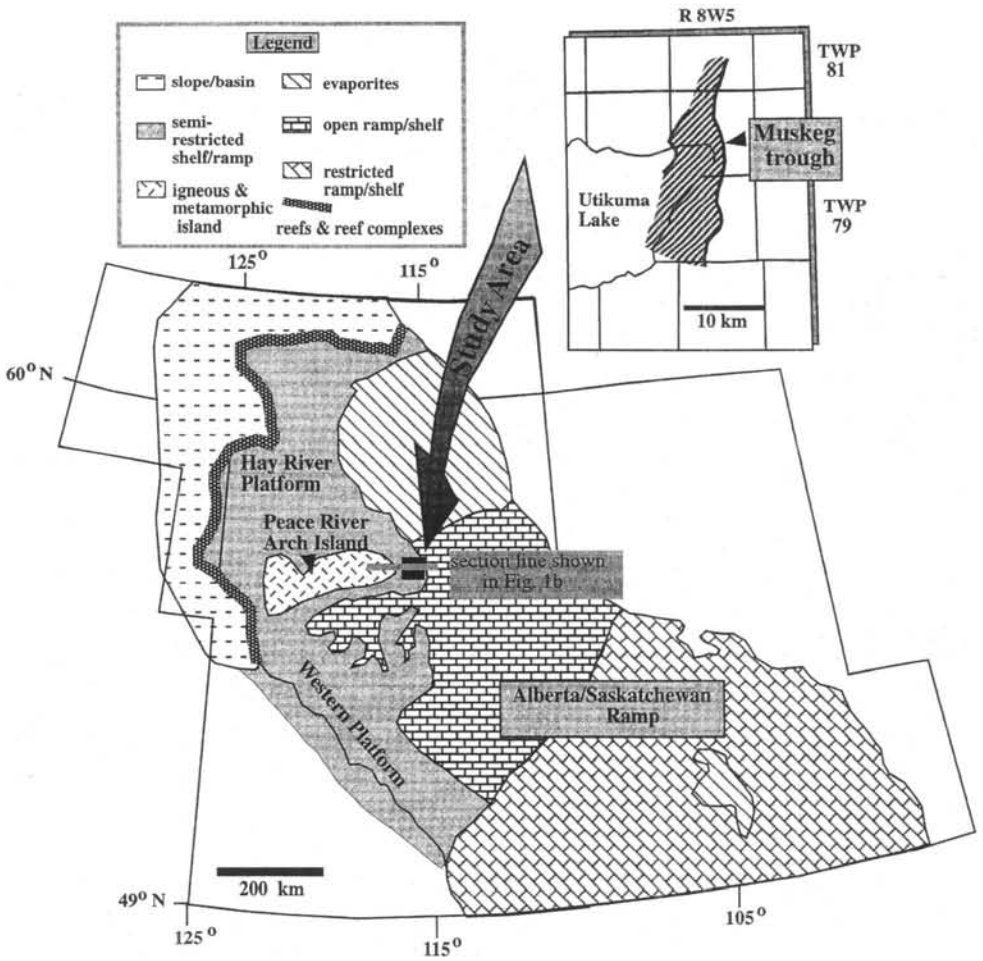

Fig. 2. Major tectonic and depositional elements of the Middle Devonian in Western Canada (modified from Moore, 1989). Enlarged map of the study area shows the location of the Muskeg Trough, a prominent topographic low during deposition of the Gilwood Member (modified from Alcock & Benteau, 1976).

Dolocretes

Nodular, argillaceous dolostones, identified herein as dolocretes, are only developed within the illitic mudstones of the Gilwood Member. They have either gradational or sharp contacts with under-and overlying lithologies. They range from completely cemented zones of structureless, microcrystalline, very well indurated dolocrete to rare, partially cemented zones with nodular forms (Fig. 5). Nodules both displace and enclose the surrounding mudstone.

Mudstones hosting dolocretes may be either dark green to greenish grey, parallel or wavy bedded to structureless, marine shales or alternatively, host mudstones may be pedogenically overprinted, alluvial floodplain deposits. Nodules may be barely visible in dry core but in wetted core commonly form spectacular, coarse, angular jigsaw fabrics with mudstone in internodular spaces.

Differences in dolocretes that are contained within marine mudstones and those in pedogenically altered floodplain mudstones are: (1) dolocretes in pedogenically altered hosts are of limited vertical and lateral extent (<0·1 m thick and not correlatable between cores, ≈0·4 km) compared to dolocretes in marine mudstone hosts, which correlate across the oil field (≈30 km) and are up to several metres thick; (2) anhydrite nodules and abundant pyrite are present in marine mudstone hosts; (3) calcite cemented, channel fill sandstones that sharply and irregularly overlie pedogenically altered floodplain mudstone hosts; and (4) rare nodules with well-rounded, well-defined edges, calcite spar-filled cracks and red mottles within pedogenically altered floodplain mudstone hosts. One of these

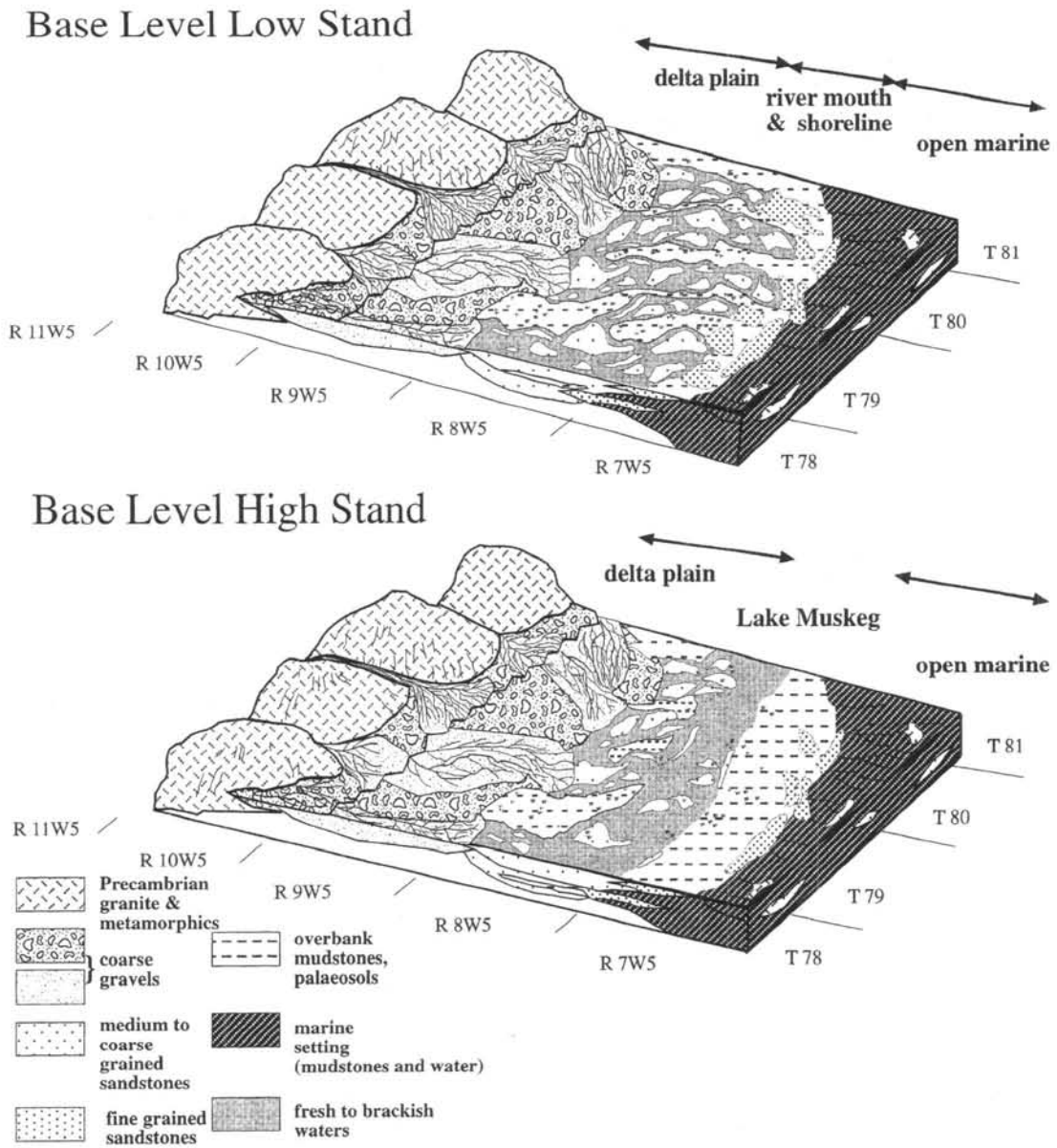

Fig. 3. Interpreted palaeogeography of the Gilwood Mbr floodplain during both base-level low stand and high stand. An escarpment to the west was the dominant source area for sediments and an alluvial-deltaic plain emptied into a large north–south trending lake that was periodically connected to the open marine setting to the east, depending on relative sea level.

nodules was sampled for carbon and oxygen isotopes and is termed a mixed dolocrete/calcrete hereafter.

Petrography and cathodoluminescence (CL)

Transmitted light petrography of calcretes and dolocretes failed to show the microfabrics and cement stratigraphy of calcite and dolomite that were clear using CL petrography. For this reason, we discuss only the CL information here.

Calcrete

Calcrete nodules show CL zoning as follows (Fig. 6): (1) Early stage subhedral crystals with non-luminescent or rarely zoned cores and bright rims (10–50 μm) that coalesce to comprise the bulk of the nodules (Fig. 6A,B & C). (2) Rare multizoned, larger (150 μm) euhedral crystals that may be cut by stylolites (Fig. 6A). (3) Circumgranular cracking, clay-filled root networks and mosaics of weakly luminescent crystals that are rimmed by

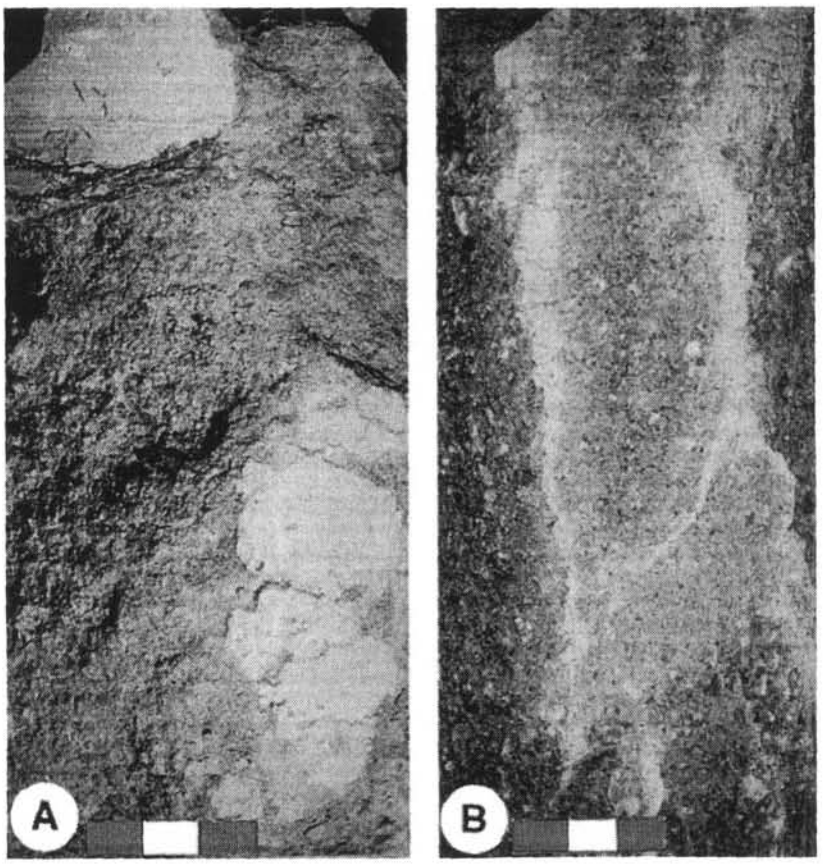

Fig. 4. Transverse view of oval and elongated calcrete nodules within both mudstone and sandstone host lithologies observed in drill core: (A) vertically stacked, displacive and horizontally elongated, oval nodules within a sandy green mudstone with multiple internodular stylolites (10-06-80–07W5, 5565 ft*); (B) vertically elongated, downward tapering and bifurcating nodules within a red and green colour mottled sandstone which are predominantly rhizogenic in origin (12-18-80-08W5, 5676·25 ft). Scale bars are 3 cm long. *Measurements in Imperial units to observe Canadian standards.

brightly luminescent cements (Fig. 6B). (4) Fossiliferous, nodular sandstone hosts, in which the walls of charophyte oogonia are darkly luminescent and micritic (Fig. 6C); void fill within the oogonia centres are comprised of a dark, to weakly luminescent, coarse spar that has a very thin (<8 μm) brightly luminescent, crenulate rim. Elongate channel voids have a similar cement fill, with central, void filling, darkly luminescent spar and thin, crenulate, luminescent rims. (5) Intergranular cements within sandstones are comprised of either bright yellow to bright orange luminescent, zoned, coarse spar (Fig. 6D) that appears to be replacing quartz grains in part. (6) Coloform fabrics associated with flower spar (Fig. 6E) are seen in well formed calcrete nodules. Several stages of calcite growth can be seen as larger voids contain both zoned crystals and spar.

Dolocretes

Dolocretes in both marine mudstone and pedogenically overprinted hosts are comprised of varying amounts of euhedral, zoned dolomite rhombs that float in a clay matrix, a planar-e texture, according to Sibley & Gregg (1987) (Fig. 7). Dolomite rhombs are commonly arranged in poorly defined circles, 0·4–1 mm in diameter. Finely disseminated pyrite is abundant and silt-sized grains of quartz and feldspar are randomly distributed in the clay matrix. Scanning electron microscopy of dolomite rhombs reveals dominantly displacive growth, as surrounding mudstones are not included within the dolomite crystals.

Mixed dolocrete/calcrete sample

CL petrography of the mixed dolocrete/calcrete sample (see above) revealed several stages of cement growth. Dolomitic nodules comprised of small (10–20 μm), brightly luminescent, subhedral crystals form the bulk of the sample (Fig. 8). Larger (80–100 μm), subhedral to anhedral dolomite rhombs, with a dark luminescent core and a bright outer edge, rim the nodules. Brown luminescent, coarse, calcite spar infills large intranodular voids. This spar contains abundant relicts of smaller (<15 μm), zoned, subhedral dolomite rhombs and a few large (0·25 mm), dark brown euhedral dolomite rhombs.

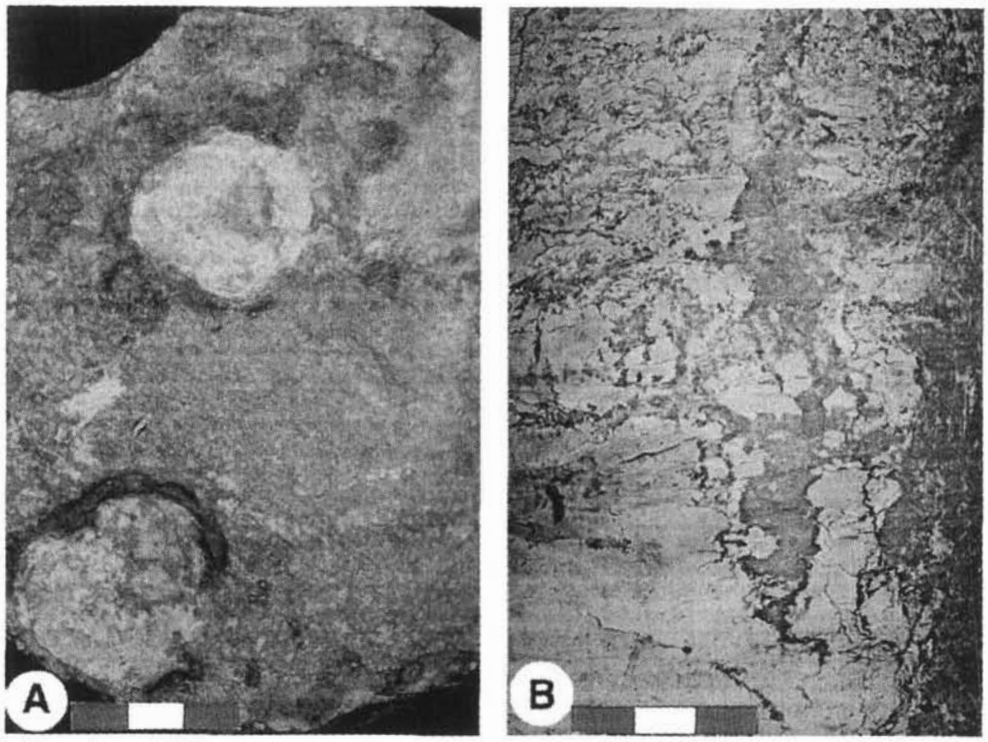

Fig. 5. (A) Plan view of dolocrete within a mudstone host with circular grey anhydrite nodules (10-29-79-0W5, 5520·30 ft). (B) Transverse view of lighter grey dolocrete nodules with partially interlocking jigsaw-like fabric within darker mudstone host (10-29-79-0W5, 5512 ft). Scale bar is 3 cm long.

Stable isotopes

Calcretes

Cross-plots of $\delta^{13}C$ and $\delta^{18}O$ values for calcretes within both mudstone and sandstone hosts plot into two distinct domains (Fig. 9A). Calcrete nodules in sandstones and mudstones have a similar range of $\delta^{13}C$ values (~ -1 to $-7‰$), but differ in their $\delta^{18}O$ values. Calcretes in sandstone hosts have $\delta^{18}O$ values between ~ -8 to $-11‰$ whereas values in mudstone hosts are between ~ -3 to $-8‰$. Calcretes in muddy sandstones have $\delta^{18}O$ values that plot in an intermediate position between these two well-defined domains. We were unable to sample sandstones at the scale needed to separate calcite nodules from adjacent intergranular spar. Therefore, calcite cemented sandstones probably reflect a mixture of values from these two sources.

Within mudstones, we found no correlation between isotope values and inferred nodule origins. That is, we were unable to distinguish between nodules that were obviously associated with rooting, versus those that were not. One calcite nodule within a mudstone has the highest $\delta^{13}C$ and $\delta^{18}O$ values (plots in the upper, right hand side of the graphed domain, Fig. 9A); it is in close proximity (10 cm above) to a dolocrete.

Dolocretes $\delta^{13}C$ and $\delta^{18}O$ values for dolocretes in marine mudstone and pedogenically altered hosts plot in two domains that are segregated mainly by differences in $\delta^{18}O$ values but have a considerable, but overlapping range in $\delta^{13}C$ values (Fig. 9B). The range in isotopic values is not obviously related to geographical location or stratigraphic position. Dolocretes in marine hosts have $\delta^{18}O$ values that range from ~ -3 to $+1‰$ with the corresponding $\delta^{13}C$ values between ~ -6 to $+3‰$. Dolocretes in pedogenically overprinted hosts have more negative $\delta^{18}O$ values (≈ 2 to $-6‰$), relative to regional dolocretes. They plot in a domain which is coincident with and overlaps calcretes within mudstone hosts.

Field relationships and distribution of calcrete and dolocrete

Calcrete and dolocrete distribution in the study area and their respective host lithologies are

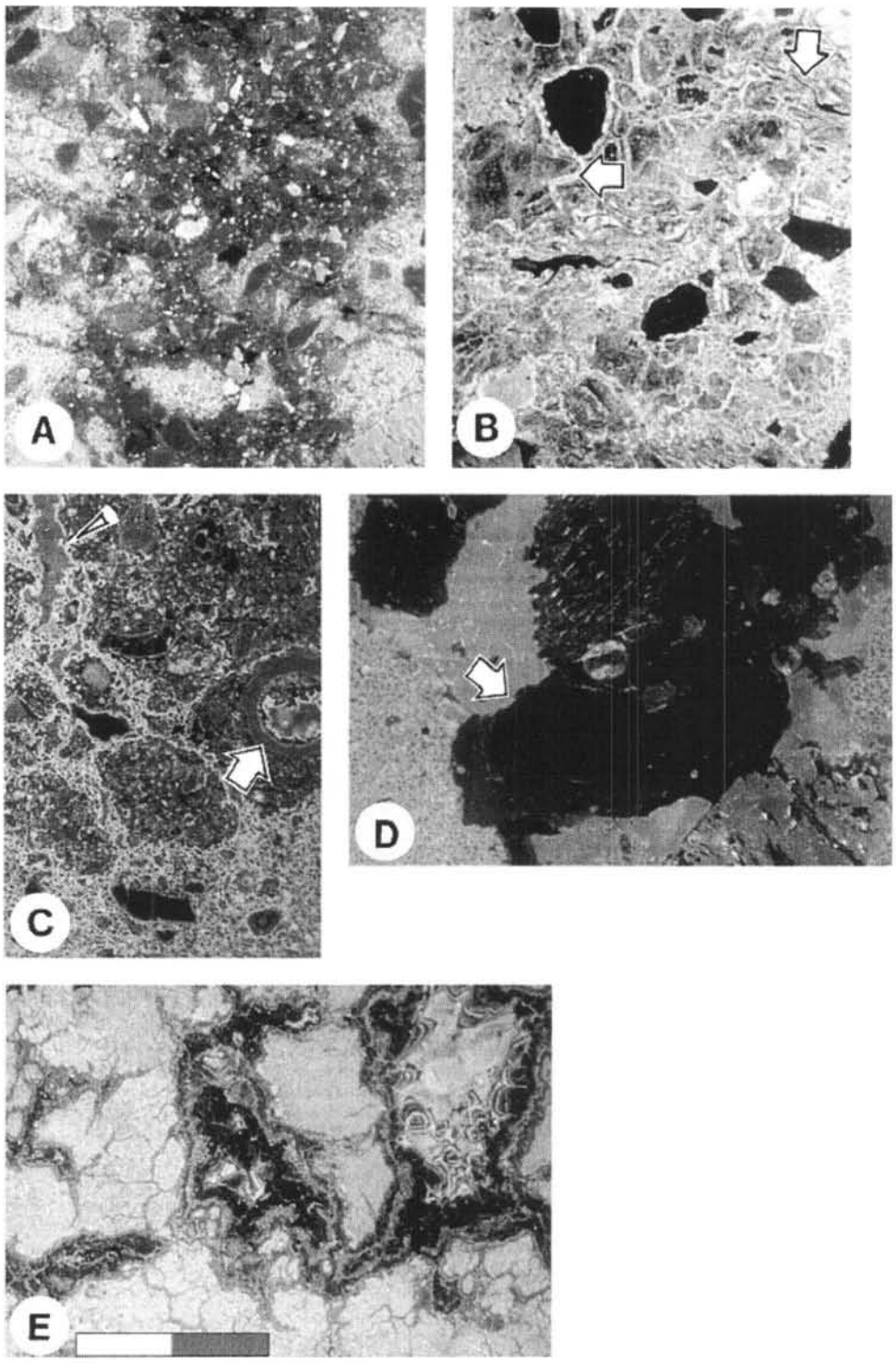

illustrated in Fig. 10. Dolocretes are found only in illitic mudstones, whereas calcretes are found in both mudstones and sandstones. In the central part of the study area, numerous, thick calcretes are present within both thick alluvial and shoreline sandstones and gleyed palaeosol mudstones. Calcretes are centred predominantly along the axis of the Muskeg Trough. Laterally extensive dolocretes are found within marginal marine to marine mudstones: (1) at the base of

Fig. 6. Stages of calcrete nodule growth as shown by cathodoluminescence (CL) petrography. Entire scale bar is 1 mm long. (A) Desiccation crack, infilled with illitic clays and silt-sized quartz (solid, medium and dark grey) and feldspar (solid, white and light grey) grains, cross-cuts a calcretized mudstone. Surrounding calcrete nodules are comprised of small subhedral crystals, with dark crystal cores and bright rims (14-16-80-08W5, 5659·5 ft). (B) Calcrete nodule with subhedral microcrystalline domains with dark and medium grey cores and bright light grey rims that contains rhizoliths and circumgranular cracks. Root structures are represented by both rhizocretions comprised of larger, weakly luminescent, subhedral microcrystal masses that are rimmed by brightly luminescent cements (arrow, centre left), and variably elongate root networks with black to dark grey, clay-filled masses outlined by bright (white and light grey) carbonate cements (arrow, upper right). Circumgranular cracking patterns pervade the sample and are associated with rhizoliths and quartz (solid, black and dark grey) and feldspar (solid, light and medium grey) grains (10-11-80-08W5, 5547·5 ft). (C) Fossiliferous calcrete within a sandstone host is comprised dominantly of small subhedral crystals with darkly luminescent or zoned cores and bright rims, and medium grey carbonate masses with clotted textures internally and bright rims. Charophyte fossil moulds (large arrow centre right) and root channel voids (small arrow top) contain bright internal isopachous rims and internal darkly luminescent to zoned, void-filling spars (14-16-80-08W5, 5659·5 ft). (D) Coarse, intergranular, zoned spar within sandstones is brightly luminescent. Carbonate rip-up clasts with microgranular calcrete similar to that detailed in A & B above are present along the periphery. Quartz and feldspar (dark grey) interdigitate with calcite as shown by crenulate calcite-feldspar contact (arrow) (10-11-80-08W5, 5547·5 ft). (E) Coloform calcrete nodule within a sandstone host that is comprised of bright luminescent carbonate that overprints many small subhedral crystals with darkly luminescent cores and bright rims. Most of the internodular space is filled with zoned to darkly luminescent isopachous spar. Larger voids contain larger euhedral zoned crystals and brightly luminescent, zoned spar (10-11-80-08W5, 5547·5 ft). Additional details in text.

the succession in the south and west central areas; and (2) throughout the area overlying the Gilwood Member, within the overlying Watt Mountain Formation. To the west, close to the highland source area for terrigenous sediments, calcretes are most common in coarser grained arkosic sandstones. East and south of the Muskeg Trough, both dolocretes and calcretes are common, and although they are not easily correlated between cores, the section is generally comprised of an alternating succession of dolocrete–calcrete.

DISCUSSION

Calcretes

Field relationships and distribution – interpretation

Carbonate sources and the processes which formed calcretes must provide an explanation for the observed field relationships and distribution. If the carbonate source was dominantly aeolian dust, then calcretes should be relatively evenly distributed throughout the alluvial plain. In contrast, if the carbonate source was mainly palustrine carbonate, then we should see some lateral and vertical association of palustrine and calcrete deposits (Colson & Cojan, 1996). If the overall distribution of carbonate was greatly affected by vegetational changes then we would expect systematic changes in carbonate nodule morphology across the alluvial plain, from the highland in the west to the marine setting to the east. Evaporation or evapotranspiration would have produced thicker accumulations of carbonate in topographically higher areas to the west that were subaerially exposed for longer periods of time (Gile *et al.*, 1966; Leeder, 1975; Ettensohn *et al.*, 1988; McFadden, 1988). As none of these field relations were seen, an alternative explanation for a carbonate source and process of formation is needed.

Calcretes in both mudstone and sandstone hosts are both common and well developed in strata to the west and within the central palaeotopographic low, the Muskeg Trough (Fig. 10). Because the distribution of calcrete deposits mimics the shape of the Muskeg Trough, we suggest that the main source of carbonate was groundwater flowing into this central low. Calcretes in both mudstones and sandstones are more common in the central part of the trough where the strata are substantially thickened. Low groundwater flux within this central area may have been created by: (1) the low relief alluvial plain (<0·05 m km^{-1}); (2) convergence of local, intermediate and regional groundwater systems at approximately the same level caused by a basal aquitard (mudstones and the Muskeg Formation); and (3) a higher sedimentation rate within the Muskeg Trough, causing a relatively low rate of meteoric water recharge. These conditions would have resulted in an alluvial plain dominated by low groundwater flux and containing high concentrations of soluble salts (Toth, 1963; Bjorlykke, 1993). Subtle changes in redox conditions, perhaps caused

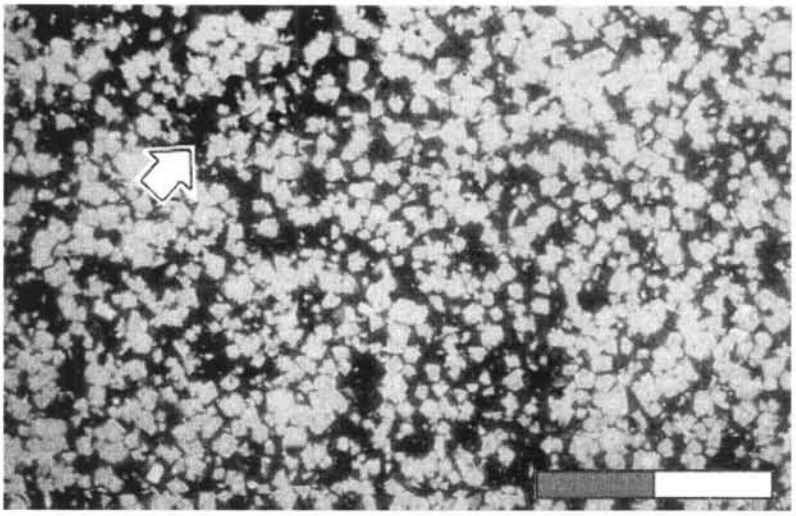

Fig. 7. Cathodoluminescence photograph of a dolocrete comprised of euhedral zoned crystals within an illitic mudstone host. Pyrite is common (arrow upper left) (10-06-81-08W5, 5486·0 ft). Entire scale bar is 1 mm.

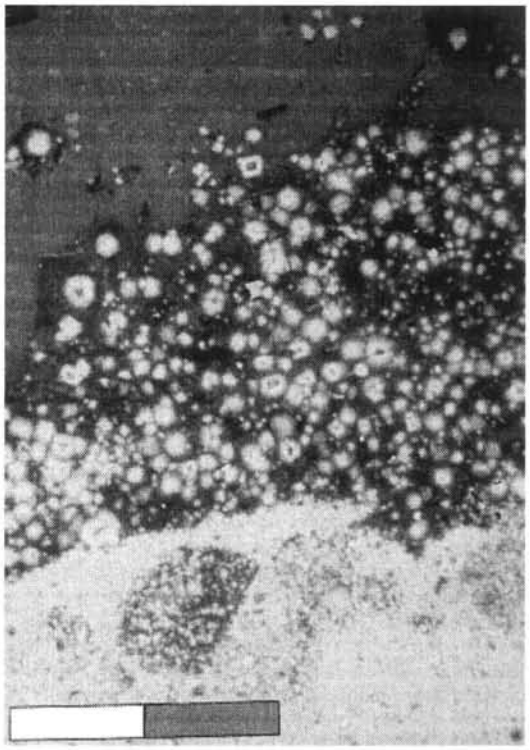

Fig. 8. The mixed dolocrete/calcrete sample with a rounded brightly luminescent nodule (bottom) comprised of small subhedral dolomite crystals with a dark core/bright rim, in gradational contact with larger, sub- to euhedral dark core/zoned rim dolomites (middle). Brown luminescent, coarse, void filling, calcite spar (top) contains both large, euhedral, dark dolomite rhombs and barely discernible relicts of dark core/bright rimmed dolomite crystals (10-06-80-07W5, 5585·4ft). Entire scale bar is 1 mm.

by changes in base level or climate, may thus have promoted mineralization. Carlisle (1983) proposed a similar groundwater source for non-pedogenic calcretes that develop along the axes of low-gradient drainages in arid climates. Porcellaneous calcretes in this setting contain pedogenic features similar to those of the Gilwood Member.

Based on reconstructed palaeotopography, the groundwater aquifer would have been sourced from the highland to the west and emptied into Lake Muskeg during relative sea-level highstands (Fig. 3). Fresh surface and ground waters would have been flowing over and through dolostones and evaporites of the underlying Muskeg Formation and therefore would have had Ca^{2+}, Mg^{2+}, CO_3^{2-}, HCO_3^- and SO_4^{2-} species in solution. During base level highstands shallow groundwaters could have calcretized the subaerially exposed, alluvial plain while terrigeneous sediments were deposited in Lake Muskeg. During base level lowstands, the lake bed was dry and sediments were subaerially exposed. The groundwater table, although still shallow, dropped below its previous level. Lithologies that had been partially cemented by groundwater calcretization during lake highstands were now subjected to vadose conditions and pedogenesis. Carbonate from groundwater and palustrine sources may have been remobilized to form pedogenic nodules.

Similar processes have been noted by Salomons & Mook (1978), where lacustrine carbonates were the source of carbonate for calcareous soils. In addition, part of the carbonate fraction present on this ancient floodplain may have been introduced by aeolian processes, as trade winds swept across carbonate platforms and ramps to the north and east (Fig. 2). Loess with particulate carbonate was probably common in the Devonian as a result of a

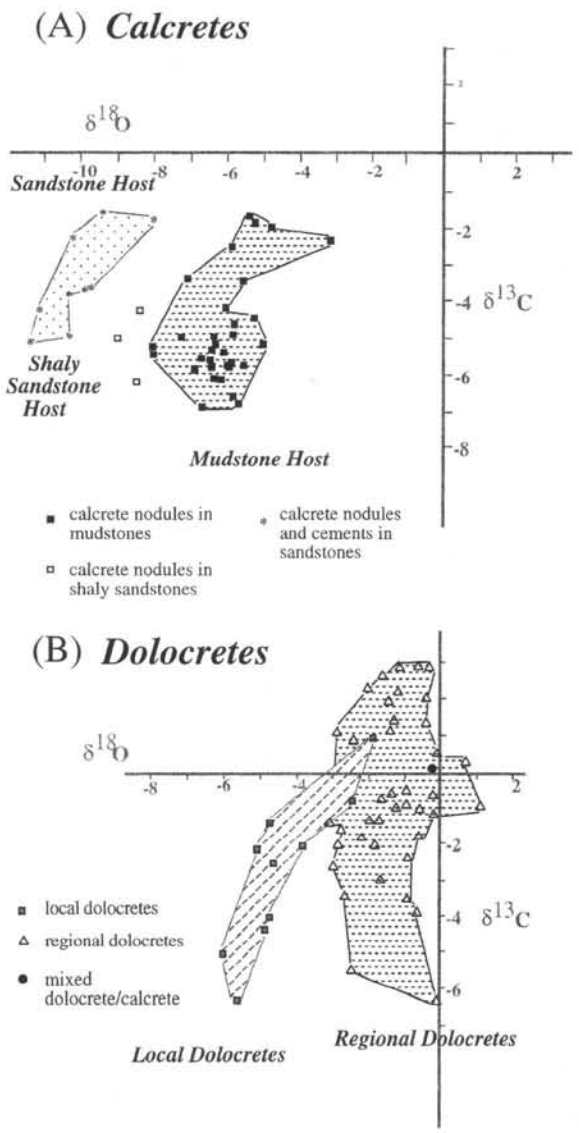

Fig. 9. Carbon and oxygen isotopes of both calcretes and dolocretes. (A) Calcrete nodules have relatively low values of both $\delta^{13}C$ and $\delta^{18}O$ and are interpreted to have formed dominantly from waters of continental origin. Calcrete nodules within mudstone hosts have higher values of $\delta^{18}O$ than those in sandstones. A gradation to lower $\delta^{18}O$ values is correlated to an increase in the sandstone content of the mudstones. (B) Local dolocretes plot in a similar domain to those of calcretes in mudstone hosts and are interpreted as derived dominantly from meteoric waters. In contrast, regional dolocretes have higher values of both $\delta^{13}C$ and $\delta^{18}O$, as a result of their origin in the mixing zone of meteoric and sea waters.

paucity of soil stabilizing vegetation compared with geologically younger settings (McPherson, 1979).

Petrography – interpretation

Much of the textural and fabric criteria published to date for distinguishing meteoric and pedogenic from phreatic carbonate (see reviews in Esteban & Klappa, 1983 and Wright & Tucker, 1991) is based on data from carbonate, rather than siliciclastic host rocks. In the dominantly siliciclastic succession of the Gilwood Member, these criteria are not easily applied. For example, petrography revealed no vadose zone cements typical of meteoric cementation (see review in Bathurst, 1975 and Esteban & Klappa, 1983), other than extremely rare flower spar (James, 1972) that is associated with coloform calcrete nodules. However, the association of calcrete nodules with desiccation cracks, illuviation features, rooting, rhizoliths, circumgranular cracks, colour mottling and siliciclastic palaeosol profiles, implies that carbonates are at least in part, pedogenic.

Despite evidence for a pedogenic origin, many features of the Gilwood Member calcretes are also indicative of groundwater processes. The calcretes are dominated by microcrystalline alpha fabrics which are common in groundwater carbonates (Wright & Tucker, 1991; Spötl & Wright, 1992). In addition they contain many features that are thought to be characteristic of groundwater carbonates such as nodular, massive and brecciated lithologies with gradational tops and abundant horizontal nodules composed of relatively small crystals (Spötl & Wright, 1992).

To explain this contradictory evidence, we propose that the siliciclastic host rocks of the Gilwood Member were affected by carbonate cementation processes within both, meteoric vadose/pedogenic and phreatic settings. Overprinting created rocks containing features common to not just one, but to all zones, as the water table fluctuated periodically. Thus, we propose that nodules formed within the meteoric vadose and pedogenic zones, the capillary transition zone and the phreatic zone, producing a cumulative cementation on the host lithologies. Determining which process occurred first, and is most highly developed within a given sample, would require more detailed work than is possible here. Instead, we suggest these carbonates are of 'dual origin' and that the resulting lithologies may contain features indicative of several different processes.

Petrography reveals several stages of calcrete cementation that was probably caused by varying redox conditions. Such variations would be common in an arid alluvial setting. They would

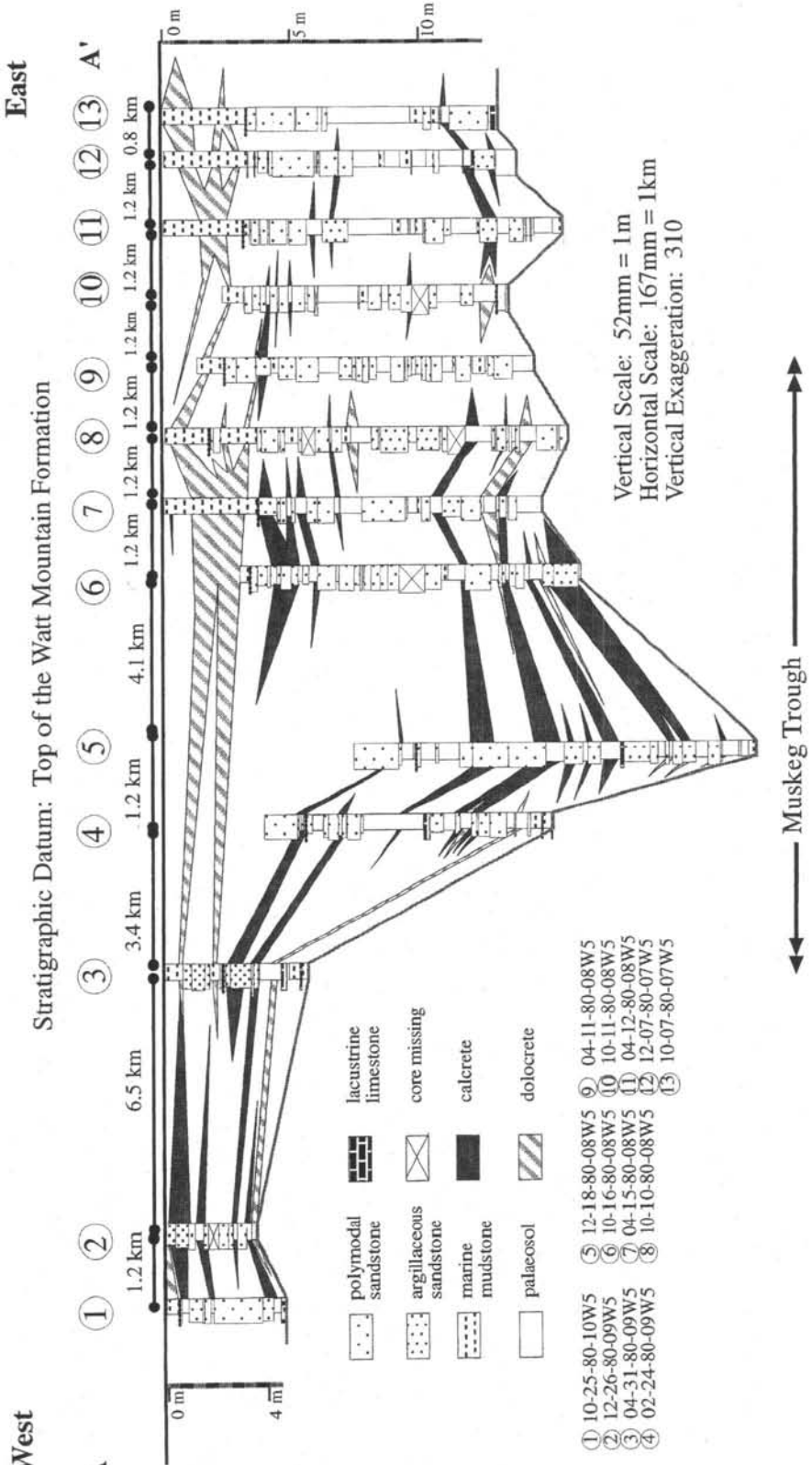
West
East
A
A'
Stratigraphic Datum: Top of the Watt Mountain Formation
1 2 3 4 5 6 7 8 9 10 11 12 13
1.2 km 6.5 km 3.4 km 1.2 km 4.1 km 1.2 km 1.2 km 1.2 km 1.2 km 1.2 km 1.2 km 1.2 km 0.8 km
0 m
4 m
0 m
5 m
10 m
polymodal sandstone
lacustrine limestone
argillaceous sandstone
core missing
marine mudstone
calcrete
palaeosol
dolocrete
① 10-25-80-10W5
② 12-26-80-09W5
③ 04-31-80-09W5
④ 02-24-80-09W5
⑤ 12-18-80-08W5
⑥ 10-16-80-08W5
⑦ 04-15-80-08W5
⑧ 10-10-80-08W5
⑨ 04-11-80-08W5
⑩ 10-11-80-08W5
⑪ 04-12-80-08W5
⑫ 12-07-80-07W5
⑬ 10-07-80-07W5
Vertical Scale: 52mm = 1m
Horizontal Scale: 167mm = 1km
Vertical Exaggeration: 310
Muskeg Trough

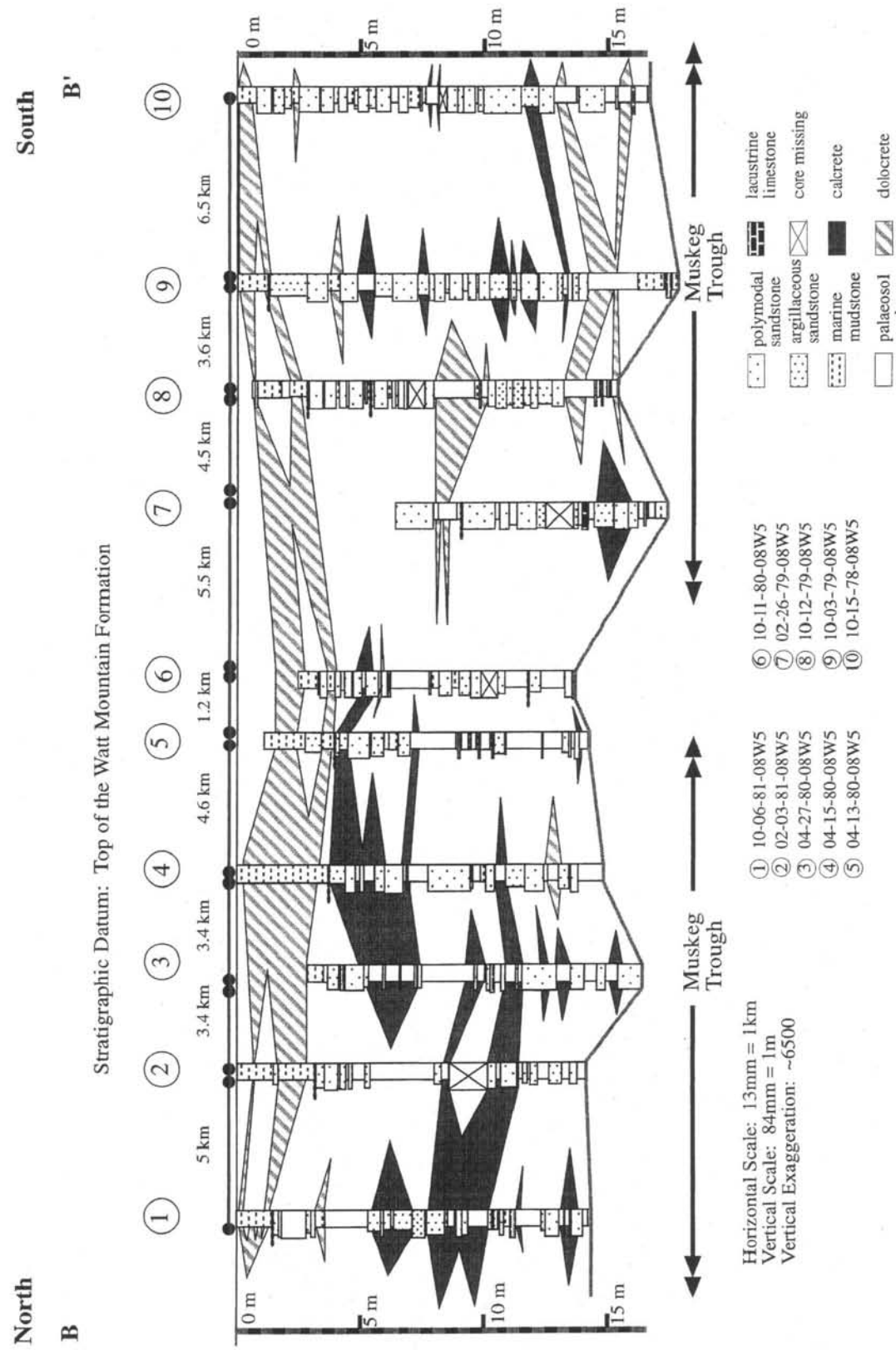

Fig. 10. West to east (A–A') and north to south (B–B') cross-sections across Nipisi field showing the distribution of host rocks, calcretes and dolocretes. Thick calcretes are centred within the thicker sandstone-mudstone succession in the Muskeg Trough. Regionally extensive dolocretes are found at the base and top of the succession within mudstone host lithologies. In general, dolocretes and calcretes to the east and south of the trough are not correlatable. Location of section lines is outlined in Fig. 1. Sections intersect at wells 04-15-80-08W5 and 10-11-80–08W5.

be caused by a fluctuating water table due to intermittent influxes of surficial water by rainfall or channel perimeter outflow. The observed pattern of luminescence, from a dark core to intermediate zoning to a bright rim has been previously interpreted as characteristic of progressive burial from meteoric to shallow phreatic settings (Frank *et al.*, 1982; Grover & Read, 1983; Frykman, 1986). It is caused by a gradual reduction in E_h during formation and the progressive substitution of first Mn^{2+} and then Fe^{2+} ions in the carbonate lattice (Meyers & Lohman, 1978; Carpenter & Oglesby, 1976).

Well-developed calcrete nodules with coloform fabrics contain several stages of cementation and may be interpreted as having formed within the fluctuating E_h–pH conditions of a meteoric to shallow phreatic zone as follows. The core of each subhedral, non-luminescent crystal would have nucleated under relatively oxidizing conditions of the vadose zone. The brightly luminescent rims were formed either during shallow burial or alternately during a rise in the water table, either of which would have created more reducing conditions within a transition to the shallow phreatic zone. Either progressive burial, or a rising groundwater table, created even more reducing conditions, in which the next stage of brightly luminescent cements formed. This was followed by cementation in a more oxidizing setting, caused during a drying out phase and a relative groundwater table fall during which coarser, less luminescent spars, were formed. Larger, zoned, darkly luminescent crystals with bright subzones postdate all of these stages and may have formed in the fluctuating E_h conditions found within the transition zone during either a subsequent groundwater table rise or progressive burial. During burial, a final stage of brightly luminescent, coarse spar may have formed in the phreatic zone.

Intergranular cements within sandstones are comprised of either bright yellow or bright orange, luminescent, zoned, coarse spar. This coarser, bright spar formed under persistent reducing conditions during burial, therefore these spars are interpreted as shallow phreatic or burial cements.

Stable isotopes – interpretation

A convincing distinction between the $\delta^{13}C$ and $\delta^{18}O$ values of lacustrine, groundwater and pedogenic calcretes has not, to our knowledge, been published. In addition, much of the modern data on pedogenic calcretes (Amundsen *et al.*, 1988; Quade *et al.*, 1989) relies on how C_3, C_4 and CAM plants fractionate carbon and is therefore of limited use in considering very ancient carbonates, particularly those of Middle Devonian age. Our isotope data plot in a similar range to calcretes from pedogenic, loess, groundwater and lacustrine settings from previous studies (Talma & Netterberg, 1983; El-Sayed *et al.*, 1991; Talbot & Kelts, 1990), pointing out the potential difficulty of distinguishing between these different types of carbonate based on isotopic data alone.

Isotope data from calcrete nodules of the Gilwood Member plot into two distinct domains (Fig. 9A). Oxygen isotopes of intergranular spars and calcite nodules within sandstones have lower $\delta^{18}O$ values relative to all other carbonates. This may be attributed to greater meteoric flushing of the more permeable sandstones relative to mudstones or alternately, due to a shallow burial origin (Dickson & Coleman, 1980; Moore, 1985; Walls *et al.*, 1979). Unfortunately, our inability to separate calcite spar from nodules within sandstones blends the isotopic signal; shaly sandstones plot in a position intermediate to the mudstone and sandstone domains because these samples contain carbonate from both sources.

Within mudstones, there is no obvious difference in isotopic values from clearly rhizogenic nodules versus those interpreted as either phreatic or pedogenic–phreatic in origin. This result is similar to the findings of Spötl & Wright (1992) on Triassic aged dolocretes.

SUMMARY

Calcretes

Based on the distribution of calcretes we believe that the main source of carbonate was groundwater, with lesser amounts supplied by aeolian and palustrine carbonates. Although we have evidence for both pedogenic and groundwater processes forming calcretes, distinguishing between these two types of carbonate is difficult using petrography and stable isotopes. Calcrete nodules associated with rooting are good evidence for pedogenesis; these carbonates, however, are probably overprinted by later phreatic processes. The similarity between pedogenic and groundwater calcretes is attibuted to frequent and marked fluctuations in the water table that created a relatively large transition zone and multiple phases of calcretization occurring within both vadose and phreatic settings.

While modern analogues for calcretes of the Gilwood Member are not common, one similar setting is found within the saline and waterlogged soils of the semiarid Indo-Gangetic alluvial floodplain (Sehgal & Stoops, 1972). Here, the interplay of groundwater and pedogenic processes has produced calcretes similar to those we describe. On this modern floodplain, nodular calcite forms are the most common type of carbonate accumulation. Another analogue was detailed by Carlisle (1983), in Western Australia and Namibia where non-pedogenic calcretes are formed in the capillary fringe zone due to evaporative processes. However, in contrast to these calcretes our Devonian examples have obvious pedogenic features which have promoted calcification of the host material.

Dolocretes

Dolocretes in marine host lithologies – interpretation

These dolocretes are similar to those interpreted as having formed within a shallow phreatic setting, or groundwater dolocretes (Khalaf, 1990; Platt & Keller, 1992; Spötl & Wright, 1992; Colson & Cojan, 1996) on the basis of their wide lateral distribution, micritic alpha fabric, brecciated and nodular character, gradational contacts, dominance of horizontal nodules and association with anhydrite nodules and pyrite. The most prominent of these dolocretes forms a laterally extensive cemented zone overlying the Gilwood Member, within the overlying Watt Mountain Formation marine mudstones. We believe it reflects a regional water table that dolocretized marginal marine to marine mudstones in a shallow phreatic setting, either just prior to or during deposition of the overlying anhydrites of the Fort Vermilion Formation. The mixing of fresher waters from the highlands to the west with marine waters encroaching from the east would have promoted dolomite formation; marine waters would have been a likely source of Mg^{2+}. Factors resulting in a low groundwater flux and hence promoting dolocretization would have been a: (1) low topographic relief caused by infill of the Muskeg Trough by this time; and (2) basal aquitard (Muskeg Formation) causing local, intermediate and regional groundwater systems to be at the same level (Toth, 1963; Bjorlykke, 1993).

Euhedral, zoned dolomite rhombs and abundant pyrite is indicative of a slightly varying, but generally low E_h during crystallization. Bacterial oxidation of organic matter and progressive burial may both cause such reducing conditions (Champ & Gullens, 1979). Isotopically, the regional dolocretes and associated calcites have the highest $\delta^{13}C$ and $\delta^{18}O$ values relative to other dolocretes. Isotopic enrichment in these carbonates is consistent with a groundwater origin and could be caused by: (1) larger amounts of preserved organic matter in the marine host mudstone (higher $\delta^{13}C$) (Williams *et al.*, 1996); (2) evaporation caused by aridity (higher $\delta^{18}O$) (Siegenthaler, 1980; Tabakh & Schreiber, 1992); (3) more highly evolved groundwater relative to meteoric water (higher $\delta^{18}O$) (Spötl & Wright, 1992); and (4) enrichment in both $\delta^{18}O$ and $\delta^{13}C$ due to less overprinting by vadose and pedogenic processes and soil-derived waters (Platt, 1989). Although the $\delta^{13}C$ values of both regional dolocretes and associated calcites are more negative than most marine organic carbon sources (cf. Degens & Epstein, 1964), it has been shown (Baker & Burns, 1985) that marine sediments can yield relatively light $\delta^{13}C$ values if they have a high primary organic content.

A suitable modern analogue for these dolocretes is difficult to find. Evaporative groundwater dolomites described by Warren (1990) and Botz & von der Borch (1984) within the Coorong lagoons of Australia, are formed by a similar process of mixed continental and sea water dolomitization (Rosen *et al.*, 1988), but in contrast, they are of limited lateral extent. Further, the $\delta^{18}O$ values of the Gilwood Member dolomite are low relative to those of the Coorong. A similar mineralogy of protodolomite and gypsum has developed within mudstones associated with a temperate, freshwater lake and mudflat system described by Nesbitt (1990), but no published isotopic data are available for these sediments. Other analogues might include Tertiary and Miocene strata (Khalaf, 1990; Armenteros *et al.*, 1995), where dolocretes have developed within mudflats and marginal lacustrine deposits and calcretes developed within sandy proximal alluvial facies.

Local dolocretes within pedogenically altered mudstone host and mixed calcretes/dolocretes – interpretation

The juxtaposition of these dolocretes with channel sandstones upsection and gradational lower contact with pedogenically altered mudstones downsection leads us to believe that these dolocretes formed within a periodically

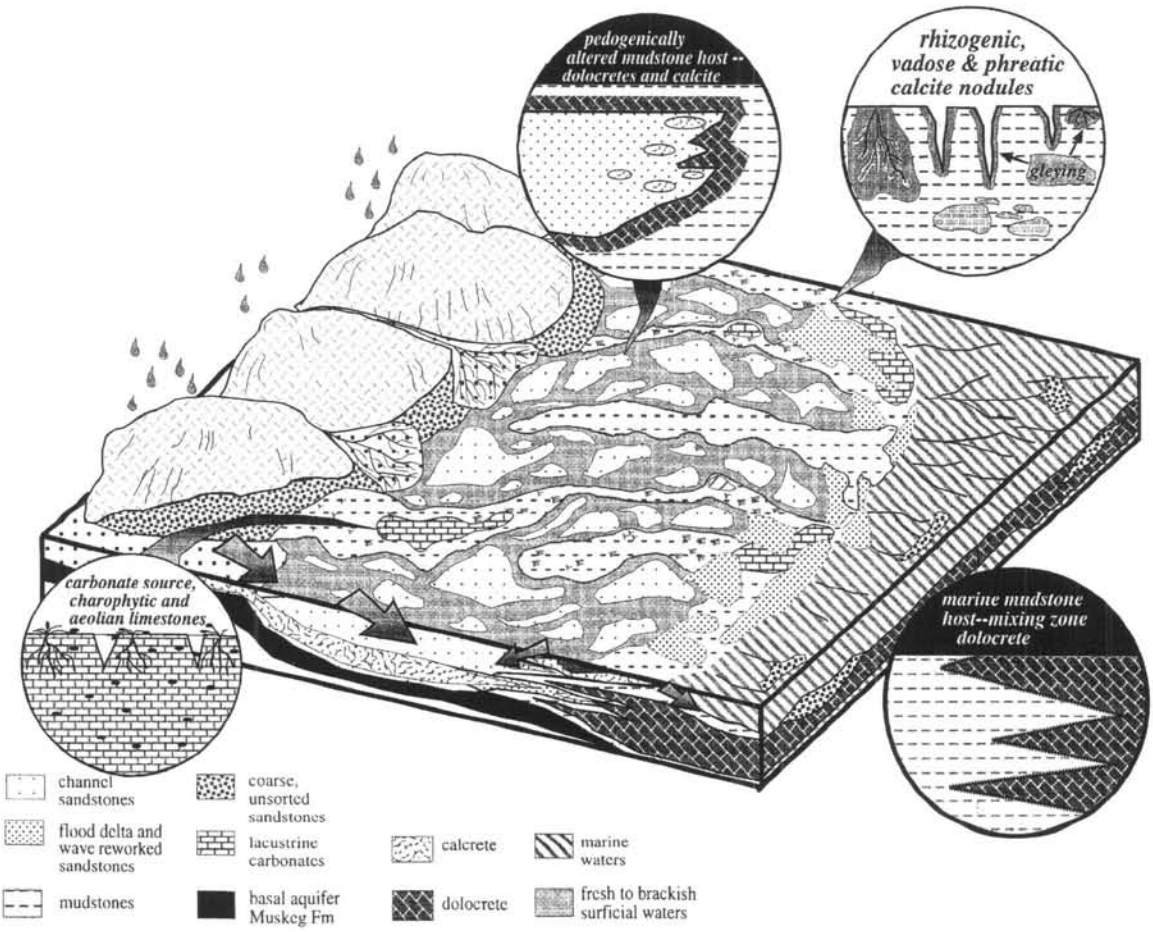

Fig. 11. Summary model depicting the vadose, pedogenic and phreatic processes that formed dolocretes and calcretes within the Gilwood Mbr. Surface and groundwaters rich in Ca^{2+}, Mg^{2+}, HCO_3^-, CO_3^{2-} and SO_4^{2-} from the highland to the west flowed towards a central topographic low and ephemeral lake caused by the Muskeg Trough. Dolocretes and calcrete nodules of limited lateral extent, formed by progressive mineralization caused by groundwater flow through and adjacent to buried, permeable, channel sandstones. Rhizogenic, vadose and phreatic calcite nodules, most abundant within the Muskeg Trough, formed within a zone of relatively sluggish groundwater flux and fluctuating surficial and groundwater tables. Fluctuations in the base level of Lake Muskeg, caused by either climatic or relative sea-level variations, resulted in pedogenic overprinting and reworking, creating calcite with both a phreatic and pedogenic origin. Laterally extensive, regional dolocretes formed by mixing zone dolomitization where the meteoric and sea-water phreatic zones interacted. Palustrine, charophytic carbonates, although minor in volume and lateral extent, may have been one source of carbonate for early diagenetic carbonate mineralization.

waterlogged horizon and are a variation of a Gley soil as described by Buurman (1980). Instead of the usual succession of a permanently waterlogged grey horizon (CG) of the phreatic zone, overlain by a mottled, partly oxidized horizon (Cg) of the transition to vadose zone, the succession is simply transposed. Thus, groundwater zonation is 'upside down' relative to a Gley soil because of groundwater flow through overlying and juxtaposed alluvial deposits.

Petrography and CL of local dolocretes is similar to that of regional dolocretes, and thus similar fluctuating E_h conditions during crystallization within a mudstone host is proposed. However, the $\delta^{13}C$ and $\delta^{18}O$ values from local dolocretes are relatively low compared to regional dolocretes, and plot in a similar domain to those of pedogenic-phreatic nodules within mudstones (Fig. 9B). This supports formation within both a groundwater and pedogenic setting from waters of similar composition to those that formed calcretes.

Mixed dolocrete–calcrete lithologies are found within the local groundwater cemented zone and overlie nodular calcitic mudstones. They are extremely rare, which indicates that the solutions from which they formed infrequently

coprecipitated both minerals. As predicted by Land (1980), these co-existing calcites and dolomites either have similar isotope values or alternatively, calcite has $\delta^{18}O$ values that are lower by 4‰ relative to dolomite. The mutual replacement of one carbonate phase for another is well demonstrated in Fig. 8.

The proposed model for local dolocrete and mixed calcrete/dolocrete formation is similar to that proposed by Arakel (1986) for palaeodrainages in Australia. However, instead of progressive mineralogical changes from calcite to dolomite in a down-dip direction, we propose this same mineralogical change from a position that was proximal to buried channel sandstones to a more distal location. Permeable sandstones probably carried the bulk of the groundwater discharge, and this resulted in abundant groundwater calcitization of these coarser grained alluvial sandstones. Precipitation of calcite within sandstones would have increased the Mg^{2+}/Ca^{2+} ratio and dolocretization occurred as groundwaters seeped into the surrounding mudstones. Rarely, these dolocretes were exposed to the vadose zone long enough for significant pedogenic features to develop.

Local dolocretization on this alluvial plain occurred because channels were probably dominated by effluent flow (away from the channel), rather than influent (toward the channel) and under flow (flow in the same direction as the channel) conditions. Characteristics of the Gilwood Member alluvial floodplain (detailed in Williams *et al.* in review) which Larkin & Sharp (1992) have identified as necessary to create dominantly effluent groundwater are: (1) low gradient; (2) low sinuosity; (3) relatively shallow depths; (4) high width to depth ratios; (5) mixed load to bed-load dominated fills; and (6) flow ephemerality.

Similar cementation processes have been reported from fluvio-marine strata of Neocomian age, where systematic compositional, isotopic and crystal size changes in siderites from proximal, coarse-grained facies to distal finer grained marine facies are attributed to differences in permeability and flow conditions in these units (Boles *et al.*, 1996).

CONCLUSIONS

1 Distribution of calcretes and dolocretes within the siliciclastic host sediments of the Gilwood Member reflects mineralization processes that were primarily controlled by floodplain topography, base level changes, groundwater lense fluctuations and host sediment characteristics. Calcretes and dolocretes were the result of a groundwater carbonate source and the interaction of groundwater, vadose and pedogenic processes. A summary of these processes is depicted in Fig. 11.

2 The main supply of carbonate for calcretization and dolocretization was by groundwater, with aeolian and palustrine carbonates supplying lesser amounts. Overprinting of host sediments by groundwater and pedogenic processes produced host lithologies with features that are associated with the meteoric/pedogenic and phreatic zones.

3 Calcrete distribution was controlled by the sluggish groundwater flow created by a: (a) prominent palaeotopographic low, the Muskeg Trough, in which ephemeral Lake Muskeg, was situated; (b) basal aquitard formed by impermeable mudstones and evaporites of the Muskeg Formation; (c) relatively high sedimentation rate within the Muskeg Trough; and (d) low relief alluvial plain.

4 Dolocretes that have a basin-wide distribution formed within marine mudstones at the base of the Gilwood Member or within the overlying Watt Mountain Formation mudstones. Mixing of fresher waters from the highland to the west and seawaters from the east resulted in dolomitization with a ready source of Mg^{2+} supplied by the marine waters.

5 Dolocretes of limited lateral extent formed within gleyed palaeosol mudstones. Horizons similar to those seen in Gley soils formed as groundwater outflow from channel sandstones affected surrounding palaeosols. Groundwater flow through permeable sandstones resulted in calcretization in channel proximal mudstones and dolomitization in channel distal mudstones.

ACKNOWLEDGMENTS

Funding for this project was provided by Amoco Canada Petroleum Company Ltd. and the National Sciences and Engineering Research Council. K. Wilde (Amoco) provided unending encouragement and thought provoking discussion. R. Strom (Amoco) is thanked for his assistance with the CL petrography. W. Yang (The University of Calgary) processed the samples for stable isotope analyses. The text benefited from the critical reviews of N. Platt, S.K. Tandon, C. Spötl, S. Burns and J. Andrews.

REFERENCES

Alcock, F.G. and Benteau, R.I. (1976) Nipisi field – a Middle Devonian clastic reservoir. In: *The Sedimentology of Selected Clastic Oil and Gas Reservoirs in Alberta.* (Ed. by M.M. Lerand), pp. 1–24. *Can. Soc. Pet. Geol.*, Calgary.

Amundsen, R.G., Chadwick, O.A., Sowers, J.M. and Doner, H.E. (1988) Relationship between climate and vegetation and the stable carbon isotope chemistry of soils in the Eastern Mojave desert, Nevada. *Quat. Res.*, **29,** 245–254.

Arakel, A.V. (1986) Evolution of calcrete in palaeodrainage of the Lake Napperby area, Central Australia. *Palaeogeog. Palaeoclim. Palaeoecol.*, **54,** 283–303.

Armenteros, I., Bustillo, M.A.A. and Blanco, J.A. (1995) Pedogenic and groundwater processes in a closed Miocene basin (northern Spain). *Sedim. Geol.*, **99,** 17–36.

Baker, P.A. and Burns, S.J. (1985) Occurrence and formation of dolomite in organic-rich continental margin sediments. *Bull. Am. Ass. Petrol. Geol.*, **69,** 1917–1930.

Bathurst, R.G.C. (1975) *Carbonate Sediments and Their Diagenesis.* Elsevier Scientific Publishing Company, New York.

Bjorlykke, K. (1993) Fluid flow in sedimentary basins. *Sedim. Geol.*, **86,** 137–158.

Boles, J.R., Hickey, J.J. and Frank, K. (1996) Occurrence of siderite in the Point McIntyre field, north slope, Alaska: an indicator of paleo aquifers. Abstract, *Annual AAPG-SEPM-EMD-DPA-DEG Conference*, San-Diego, A17–A18.

Botz, R.W. and von der Borch, C.C. (1984) Stable isotope study of carbonate sediments from the Coorong area, South Australia. *Sedimentology*, **31,** 837–849.

Burwash, R.A. (1957) Reconnaissance of subsurface Precambrian of Alberta. *Bull. Am. Ass. Petrol. Geol.*, **41,** 70–103.

Buurman, P. (1980) Palaeosols in the Reading Beds (Palaeocene) of Alum Bay, Isle of Wight, UK. *Sedimentology*, **27,** 593–606.

Carlisle, D. (1983) Concentration of uranium and vanadium in calcretes and gypcretes. In: *Residual Deposits: Surface Related Weathering Processes and Materials* (Ed. by R.C.L. Wilson), *Geol. Soc. London Spec. Publ.*, **11,** 185–195.

Carpenter, A.B. and Oglesby, T.W. (1976) A model for the formation of luminescently zoned calcite cements and its implications. *Geol. Soc. Am., Abs. with Programs*, **8,** 469–470.

Chadwick, O.A. and Nettleton, W.D. (1990) Micromorphologic evidence of adhesive and cohesive forces in soil cementation. *Dev. Soil Sci.*, **19,** 207–212.

Champ, D.R. and Gullens, J. (1979) Oxidation-reduction sequences in groundwater flow systems. *Can. J. Earth Sci.*, **16,** 12–23.

Colson, J. and Cojan, I. (1996) Groundwater dolocretes in a lake-marginal environment: an alternative model for dolocrete formation in continental settings (Danian of the Provence Basin France). *Sedimentology*, **43,** 175–188.

Degens, E.T. and Epstein, S. (1964) Oxygen and carbon isotope ratios in coexisting calcites and dolomites from recent and ancient sediments. *Geochim. Cosmochim. Acta*, **28,** 23–44.

Dickson, J.A.D. and Coleman, M.L. (1980) Changes in carbon and oxygen isotope composition during limestone diagenesis. *Sedimentology*, **27,** 107–118.

El-Sayed, M.I., Fairchild, I.J. and Spiro, B. (1991) Kuwaiti dolocrete: petrology, geochemistry and groundwater origin. *Sedim. Geol.*, **73,** 59–75.

Esteban, M. and Klappa, C.F. (1983) Subaerial exposure environment. In: *Carbonate Depositional Environments* (Ed. by P.A. Scholle, D.G. Bebout and C.H. Moore). *Am. Ass. Pet. Geol. Mem.*, **33,** 1–63.

Ettensohn, F.R., Dever, G.R. Jr and Grow, J.S. (1988) A paleosol interpretation of profiles exhibiting subaerial exposure 'crusts' from the Mississippian of the Appalachian Basin. *Geol. Soc. Am. Spec. Paper*, **216,** 49–79.

Frank, J.R., Carpenter, A.B. and Oglesby, T.W. (1982) Cathodoluminescence and composition of calcite cement in the Taum Sauk Limestone (Upper Cambrian), southeast Missouri. *J. Sedim. Petrol.*, **52,** 631–638.

Freytet, P. and Plaziat, J.S. (1982) Continental carbonate sedimentation and pedogenesis-Late Cretaceous and Early Tertiary of Southern France. *Contributions to Sedimentology*, **12.** Springer-Verlag, Stuttgart.

Frykman, P. (1986) Diagenesis of Silurian bioherms in the Klinteburg Formation, Gotland, Sweden. In: *Reef Diagenesis* (Ed. by J.H. Schroeder and B.H. Purser), pp. 399–423. Springer-Verlag, Berlin.

Gile, L.H., Peterson, F.F. and Grossman, R.B. (1966) Morphological and genetic sequences of carbonate accumulation in desert soils. *Soil Sci.*, **101,** 347–360.

Goudie, A.S. (1973) *Duricrusts in Tropical and Subtropical Landscapes.* Clarendon Press, Oxford.

Grover, G. and Read, J.F. (1983) Paleoaquifer and deep burial related cement defined by regional cathodoluminescent patterns, Middle Ordovician carbonates, Virginia. *Bull. Am. Ass. Pet. Geol.*, **67,** 1275–1303.

Habicht, J.K.A. (1979) Paleoclimate, paleomagnetism and continental drift. *Am. Ass. Pet. Geol., Studies Geol.*, **9,** 31.

James, N.P. (1972) Holocene and Pleistocene calcareous crusts (caliche) profiles: indicators of near-surface subaerial diagenesis, Barbados, West Indies. *Bull. Can. Pet. Geol.*, **25,** 123–173.

Khalaf, F.I. (1990) Occurrence of phreatic dolocrete within Tertiary clastic deposits of Kuwait, Arabian Gulf. *Sedim. Geol.*, **68,** 223–239.

Klappa, C.F. (1980) Rhizoliths in terrestrial carbonates: classification, recognition, genesis and significance. *Sedimentology*, **27,** 613–629.

Klingspor, A.M. (1969) Middle Devonian Muskeg evaporites of Western Canada. *Bull. Am. Ass. Pet. Geol.*, **53,** 927–948.

Land, L.S. (1970) Phreatic versus vadose meteoric diagenesis of limestones: evidence from a fossil water table. *Sedimentology*, **14,** 175–185.

Land, L.S. (1980) The isotopic and trace element geochemistry of dolomite: the state of the art. In:

Concepts and Models of Dolomitization (Ed. by D.H. Zenger, J.B. Dunham and R.L. Ethington). *SEPM Special Publication*, **28,** 87–110.

Larkin, R.G. and Sharp, J.M. (1992) On the relationship between river-basin geomorphology, aquifer hydraulics, and ground-water flow direction in alluvial aquifers. *Geol. Soc. Am. Bull.*, **104,** 1608–1620.

Leeder, M.R. (1975) Pedogenic carbonates and flood sediment accretion rates: a quantitative model for alluvial arid-zone lithofacies. *Geol. Mag.*, **112,** 257–270.

Mack, G.H., James, W.C. and Monger, H.C. (1993) Classification of paleosols. *Geol. Soc. Am. Bull.*, **105,** 129–136.

McCrea, J.M. (1950) The isotopic chemistry of carbonates and a paleotemperature scale. *J. Chem. Phys.*, **18,** 849–857.

McFadden, L.D. (1988) Climatic influences on rates and processes of soil development in Quaternary deposits of southern California. *Geol. Soc. Am. Spec. Paper*, **216,** 153–177.

McPherson, J.G. (1979) Calcrete (Caliche) palaeosols in fluvial redbeds of the Aztec siltstone (Upper Devonian), southern Victoria Land, Antarctica. *Sedim. Geol.*, **22,** 267–285.

Meijer-Drees, N.C. (1994) Devonian Elk Point Group of the Western Canada Sedimentary Basin. In: *Geological Atlas of the Western Canada Sedimentary Basin* (Ed. by G.D. Mossop and I. Shetsen), pp. 129–148. *Can. Soc. Pet. Geol. & Alberta Res. Counc.*, Calgary.

Meyers, W.J. and Lohman, K.C. (1978) Microdolomite-rich syntaxial cements: proposed meteoric-marine mixing zone phreatic cements from Mississippian limestones, New Mexico. *J. Sedim. Petrol.*, **48,** 475–488.

Molenaar, N. (1984) Palaeopedogenic features and their palaeoclimatological significance for the Nevremont Formation (Lower Givetian), the northern Ardennes, Belgium. *Palaeogeog. Palaeclim. Palaeoecol.*, **46,** 325–344.

Moore, C.H. (1985) Upper Jurassic cements: a case history. In: *Carbonate Cements.* (Ed. by N. Schneidermann and P.M. Harris). *Soc. Econ. Paleontol. Mineral Spec, Publ.*, **36,** 291–308.

Moore, D.M. and Reynolds, R.C. Jr (1989) *X-Ray Diffraction and the Identification and Analysis of Clay Minerals.* Oxford University Press, New York.

Moore, P.F. (1989) The Kaskaskia sequence: reefs, platforms and foredeeps, the Lower Kaskaskia sequence – Devonian. In: *Western Canada Sedimentary Basin, A Case History* (Ed. by B.D. Ricketts), pp. 139–164. *Can. Soc. Pet. Geol.*, Calgary.

Nesbitt, H.W. (1990) Groundwater evolution, authigenic carbonates and sulphates, of the Basque Lake no. 2 Basin, Canada. In: *Fluid–mineral Interactions* (Ed. by R.J. Spencer and I.M. Chou), *Geochem. Soc. Spec. Pub.*, **2,** 355–368.

Netterberg, F. (1969) The interpretation of some basic calcrete types. *S. Afr. Archael. Bull.*, **24,** 117–122.

Oldale, H.S. and Munday, R.J. (1994) Devonian Beaverhill Lake Group of the Western Canada Sedimentary Basin. In: *Geological Atlas of the Western Canada Sedimentary Basin* (Ed. by G.D. Mossop and I. Shetsen), pp. 149–163. Can. Soc. Pet. Geol. & Alberta Res. Counc., Calgary., Calgary.

Pimentel, N.L., Wright, V.P. and Azevedo, T.M. (1996) Distinguishing early groundwater alteration effects from pedogenesis in ancient alluvial basins: examples from the Palaeogene of southern Portugal. *Sedim. Geol.*, **105,** 1–10.

Platt, N.H. (1989) Lacustrine carbonates and pedogenesis: sedimentology and origin of palustrine deposits from the Early Cretaceous Rupelo Formation, W Cameros Basin, N Spain. *Sedimentology*, **36,** 665–684.

Platt, N.H. and Keller, B. (1992) Distal alluvial deposits in a foreland basin setting – the Lower Freshwater Molasse (Lower Miocene), Switzerland: sedimentology, architecture and paleosols. *Sedimentology*, **39,** 545–565.

Pugh, D.C. (1973) Subsurface Lower Paleozoic stratigraphy in northern and central Alberta. *Geol. Surv. Can., Paper* **72–12.**

Quade, J., Cerling, T.E. and Bowman, J.R. (1989) Systematic variations in carbon and oxygen composition of pedogenic carbonate along elevation transects in the southern Great Basin, United States. *Geol. Soc. Am. Bull.*, **101,** 464–475.

Rosen, M.R., Miser, D.E. and Warren, J.K. (1988) Sedimentology, mineralogy, and isotope analysis of Pellet Lake, Coorong region, South Australia. *Sedimentology*, **35,** 105–122.

Salomons, W. and Mook, W.G. (1978) Isotopic geochemistry of carbonate dissolution and reprecipitation in soils. *Soil Sci.*, **122,** 15–24.

Schuchert, C. (1976) Climates of geologic time. In: *Paleobiogeography* (Ed. by C.A. Ross), pp. 367–383. Dowden, Hutchinson and Ross, Stroudsberg, Pennsylvanian.

Scotese, C.R., Snelson, S., Ross, W.C. and Dodge, L.P. (1981) A computer animation of continental drift. In: *Global Reconstruction and the Geomagnetic Field during the Paleoozoic* (Ed. by M.W. McElhinny, A.N. Khramove, M. Ozima, M. & D.A. Valencio). *Adv. Earth Planet. Sci.*, **10,** 61–70.

Sehgal, J.L. and Stoops, G. (1972) Pedogenic calcite accumulation in arid and semi-arid regions of the Indo-Gangetic alluvial plain of erstwhile Punjab (India) – their morphology and origin. *Gedmab*, **8,** 59–72.

Sibley, D.F. and Gregg, J.M. (1987). Classification of dolomite rock texture. *J. Sedim. Petrol.*, **57,** 967–975.

Siegenthaler, U. (1980) Stable hydrogen and oxygen isotopes in the water cycle. In: *Lectures in Isotope Geology.* (Ed. by E. Jaeger and J.C. Hunziker), pp. 264–273. Springer-Verlag, Berlin,.

Spötl, C. and Wright, V.P. (1992) Groundwater dolocretes from the Upper Triassic of the Paris Basin, France: a case study of an arid, continental diagenetic facies. *Sedimentology*, **39,** 1119–1136.

Strakhov, N.E. (1970) *Principles of Lithogenesis*, **3** (Ed. by S.E. Tomkeieff and J.E. Hemingway). Plenum Publishing Corporation, New York.

Tabakh, M.E. and Schreiber, C. (1992) Lithologies and diagenesis of the lacustrine sediments of the

Lockatong Formation (Upper Triassic) in the Newark Rift Basin. In: *Lacustrine Reservoirs and Depositional Systems* (Ed. by A.J. Lomando, C. Schreiber and P.M. Harris). *SEPM Core Workshop*, **19,** 239–295.

Talbot, M.R. and Kelts, K. (1990) Paleolimnological signatures from carbon and oxygen isotopic ratios in carbonates from organic carbon-rich lacustrine sediments. *AAPG Memoir*, **50,** 99–112.

Talma, A.S. and Netterberg, F. (1983) Stable isotope abundances in calcretes. In: *Residual Deposits: Surface Related Weathering Processes and Materials* (Ed. by R.C.L Wilson), pp. 229–282, *Geol. Soc. London*, Blackwell Scientific Publications, Oxford.

Thachuk, N.M. (1968) Geological study of the Middle Devonian Gilwood arkoses in the Nipisi area, Alberta. *J. Can. Petrol. Technol.*, **7,** 181–194.

Thortenson, D.C., Mackenzie, F.T. and Ristvet, B.L. (1972) Experimental vadose and phreatic cementation of skeletal carbonate sand. *J. Sedim. Petrol.*, **42,** 162–167.

Toth, J. (1963). A theoretical analysis of groundwater flow in small drainage basins. *J. Geophys. Res.*, **68,** 4795–4812.

Tucker, M.E. and Wright, V.P. (1990) *Carbonate Sedimentology*. Blackwell Scientific Publications, Oxford.

Walls, R.A., Mountjoy, E.W. and Fritz, P. (1979) Isotopic composition and diagenetic history of carbonate cements in Devonian Golden Spike reef, Alberta, Canada. *Bull. Geol. Soc. Am.*, **90,** 963–982.

Warren, J.K. (1990) Sedimentology and mineralogy of dolomitic Coorong Lakes, south Australia. *J. Sedim. Petrol.* **60,** 843–858.

Watts, N.L. (1978) Displacive calcite: evidence from Recent and ancient calcretes. *Glgyb*, **6,** 699–703.

Wieder, M. and Yaalon, D.H. (1974) Effect of matrix composition on carbonate nodule crystallization. *Gedmab*, **11,** 95–121.

Williams, C.A., Hills, L.V. and Krause, F.F. (1996) Preserved organic matter and miospores in buried Middle Devonian (Givetian) paleosols: indicators of weathering, oxidation and maturity. *Catena*, **28,** 1–19.

Witzke, B.J. and Heckel, P.H. (1988) Paleoclimatic indicators and inferred paleolatitudes of Euramerica. In: *Devonian of the World, Proceedings of the Second International Symposium on the Devonian System* (Ed. by N.J. McMillan, A.F. Embry and D.J. Glass), pp. 49–63. *Can. Soc. Pet. Geol.*, Calgary.

Wright, V.P. and Tucker, M.E. (1991) Calcretes: an introduction. In: *Calcretes* (Ed. by V.P. Wright, & M.E. Tucker), *Int. Ass. Sed., Reprint Series*, **2,** 1–22.

Wright, V.P., Platt, N.H., Marriott, S.B. and Beck, V.H. (1995) A classification of rhizogenic (root-formed) calcretes, with examples from the Upper Jurassic–Lower Cretaceous of Spain and Upper Cretaceous of southern France. *Sedim. Geol.*, **100,** 143–158.

Yaalon, D.H. and Singer, S. (1974) Vertical variation in strength and porosity of calcrete (Nari) on chalk, Shefela, Israel, and interpretation of its origin. *J. Sedim. Petrol.*, **44,** 1016–1023.

Ziegler, P.A. (1988) Laurussia – the old red continent. In: *Devonian of the World: Proceedings of the Second International Symposium on the Devonian System* (Ed. by N.J. McMillan, A.F. Embry, A.F. & D.J. Glass), pp. 15–48. *Can. Soc. Pet. Geol.*, Calgary.

Manuscript received 19 May 1997; revision accepted 18 February 1998.